

Performance Analysis of Multiple Configurations of Passenger Vehicle Front Bumpers for Low Speed Impact

¹Amruth C H, ²Sudheer Kumar B N, ³Harsha G O, ⁴Anuradha Bhandary

¹Assistant Professor, Department of Mechanical Engineering, SSE, Mukka, Mangalore, India

²Head of the Department, Department of Mechanical Engineering, SDIT, Mangalore, India

³Assistant Professor, Department of Mechanical Engineering, SDIT, Mangalore, India

⁴Assistant Professor, Department of Mechanical Engineering, SDIT, Mangalore, India

Abstract: low speed frontal impact is the most regularly occurring scenario in the real world driving. The bumper which are basically designed to absorb crash energy and crush during high speed impact need to actually behave more rigid at low speed impacts else the damage caused to bumper is very high and will add to cost of repair and replacement. To address this issue the IIHS provides the guidelines for evaluation of bumper during low speed impacts upto 10 kmph. On IIHS guidelines, multiple bumper design configuration with weld information and analysed the performances at low speed frontal impact with energy observed and displacement point of view.

Keywords: IIHS (Insurance Institute for Highway Safety Standard, Finite Element Analysis, Bumper, Energy Observed, Displacement, Hyperview, LS Dyna.

1. INTRODUCTION

There were 16.4 million motor vehicle crashes in the U.S. Of these, 13.5 million (82 percent) were property-damage-only crashes; no occupant injury occurred. These collisions, which can be considered relatively minor, caused an average of \$1,484 of vehicle damage per crash, and cost society an estimated total of \$59.9 billion. In the United Kingdom, insurer's report the total annual cost of motor vehicle insurance is in the region of \$10 billion. About 70% of these costs are related to damage repairs in low speed crashes, with an average of \$2,000 damage per incident (Association of British Insurers). Reducing vehicle damages in low speed crashes could have a massive global financial benefit. Many of these relatively minor crashes take the form of low speed front or rear impacts. Vehicle bumper systems should be able to absorb the energy of these collisions, preventing damage to more expensive parts. Unfortunately, most bumpers are designed to meet only the minimum standards required by the regulatory body for any given market. As a result new designs are regularly introduced which pass current bumper standards and evaluation tests, but which still allow thousands of dollars in damage in minor collisions. Existing test procedures are not motivating manufacturers to improve these bumper designs. So to lower damage and easy reparability/replacements are the desirable characters of any Bumper system in passenger vehicle. The costs involved in repairing or replacing are important concerns to vehicle insurance companies, customers and vehicle manufactures. This has established a strong reason for evaluating the extent of damage caused to bumper system which is most prone to damage during an event of low speed impact under city driving conditions.

1.1 Problem Identification

Study of automotive bumper system for damageability and energy absorption characteristics of materials for low speed impact by FEA approach. To evaluate the energy management and deformation pattern of different bumper rails design. Bumpers can be designed in various ways to withstand crashes both High speed impact and low speed impact. The Bumper assembly is divided into two sub assemblies. The Bumper fascia consisting of the outer plastic components sch as bumper grille, the front bumper plastic substrate headlamps etc. The Bumper Structure consisting of the Impact bar and the crash can assembly. Here, in this project we will consider the Crash Can Assembly for the analysis – this assembly consisting of the top and bottom crash can rails are basically tubular structures and are expected to play the following roles :

To crumple completely in high speed impacts and thus absorb energy

To withstand low speed impacts without too much deformation

2. MODEL SETUP

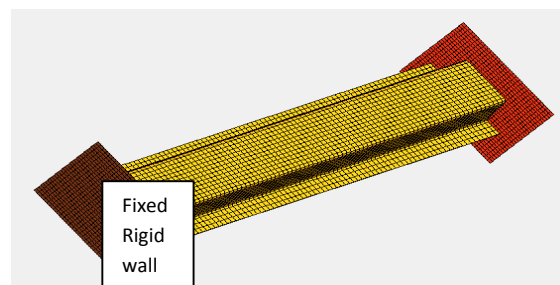


Figure 1: Base Model setup

The model set up is as shown in above figure. The base model consists of the crash can assembly made up of the top and bottom components. The assembly is fixed at one end with a fixed rigid wall which simulates the welded components attaching to the crash

can assembly. The impact is simulated using the moving rigid wall which crushes the crash can. The moving rigid wall is given motion by means of a prescribed boundary motion which refers to a load-curve.

2.1 Thickness of Rail Parts

2.2 Upper and Bottom Rails

Thickness----1.800, Thickness ---- 0.650

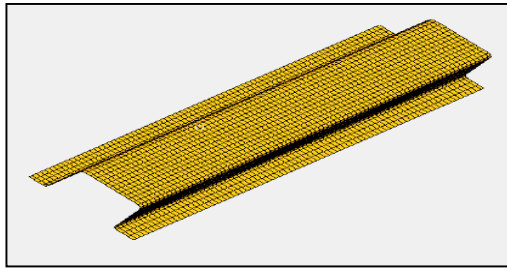


Figure 2: Top rail of crash can assembly

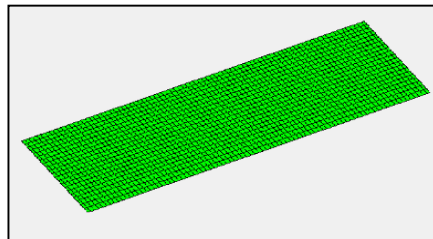


Figure 3: Base rail of crash can assembly

2.3 Two Rigid Supports One Fixed and One Moving

Thickness ----- 1.000, Thickness ----- 10.000

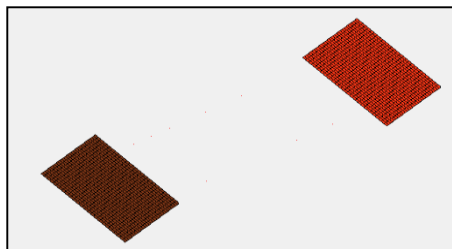


Figure 4: Two rigid supports of crash can assembly

2.4 Spot Welds Definition

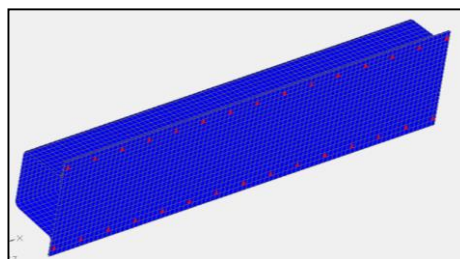


Figure 5: shows the 1D beams connected (spot welds)

The Top and bottom rails are connected to each other by means of Spot welds which are represented by 1-D Beams. The Spot welds are generated by defining a contact *CONTACT_SPOTWELD between the beams and the shells of the two parts, where the beams are slaves and the shells are master

2.5 Connection between Rigid Walls and Rails

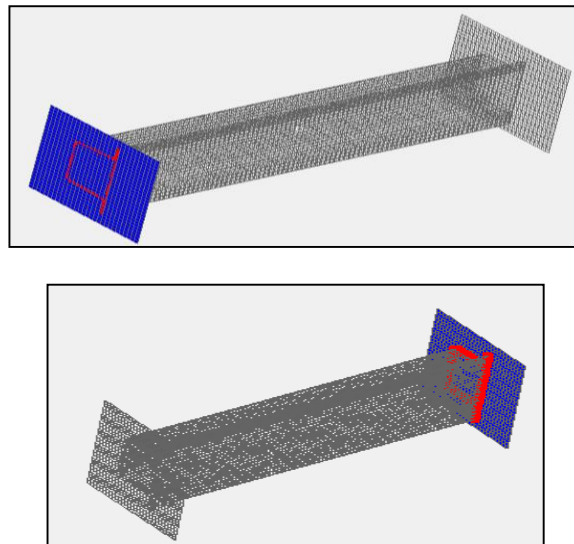


Figure 6: shows the connection between rigid walls and rails

The end nodes of the Top and Bottom rails are connected to each of the Rigid walls as shown in image by means of *CONSTRAINED_EXTRA NODE card where the nodes of the rails are slave to the master Rigid wall shells

2.6 Boundary Initial Conditions and Load Application

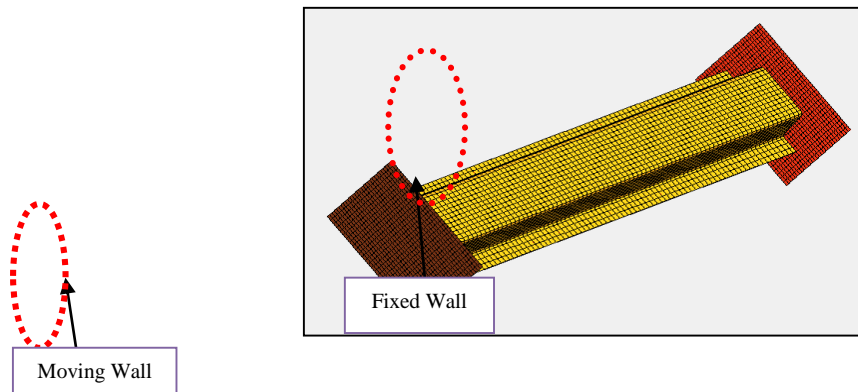


Figure 7: shows the application of Boundary conditions

The model is as shown in figure. The rails are connected to each other by means of beam spot welds, which are represented by beam elements and contact is defined between the beam elements and the rail component elements. The rigid wall elements are connected to the rails by means of extra nodes. One rigid wall is kept fixed and the other rigid wall is defined a prescribed boundary motion as it moves forward to crush the rails

2.7 Boundary Conditions

The Fixed Rigid wall has MAT 20 Rigid card constrained in all directions. The moving Rigid wall has MAT 20 Rigid card fixed in Y and Z translation directions and Free in X translational direction

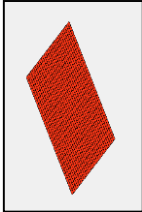
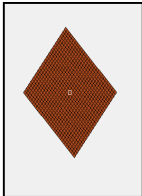
	<pre> MAT_RIGID 204 7.900e-06 205.900 0.300 0.000 0.000 0.00 0. [CMD] [CON1] [CON2] 1.0 7 7 [A1] [A2] [A3] [V1] [V2] [V3] 0.000 0.000 0.000 0.000 0.000 0.000 </pre>
	<pre> MAT_RIGID 205 7.900e-06 205.900 0.296 0.000 0.000 0.00 0. [CMD] [CON1] [CON2] 1.0 5 7 [A1] [A2] [A3] [V1] [V2] [V3] 0.000 0.000 0.000 0.000 0.000 0.000 </pre>

Figure 8: shows the assigning of material properties two crash can rigid parts

2.8 Load Application

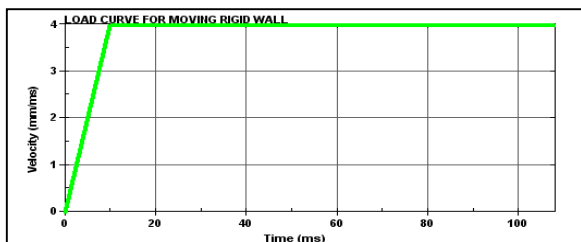
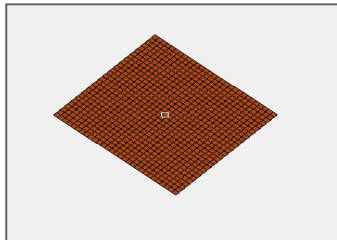


Figure 9: shows the graph of load curve for moving rigid wall

2.9 Model Details

Iteration 1 Details:

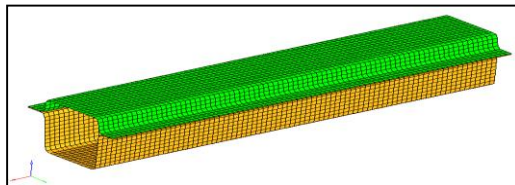


Figure 10: Cross section View of Iteration 1

Iteration 2 Details:

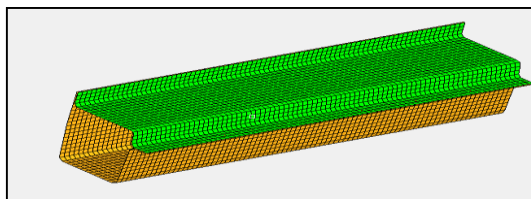


Figure 11: Cross section View of Iteration 2

Iteration 3 Details:

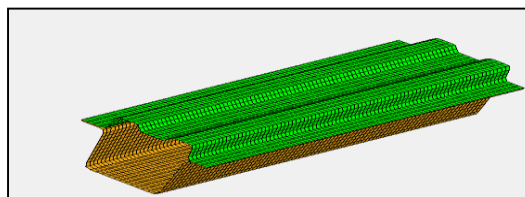


Figure 12: Cross section View of Iteration 3

Iteration 4 Details:

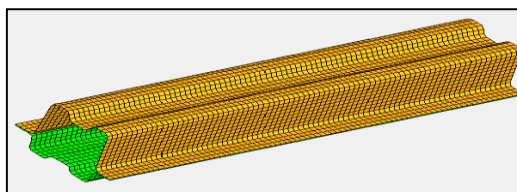


Figure 13: Cross section View of Iteration 4

Iteration 5 Details:

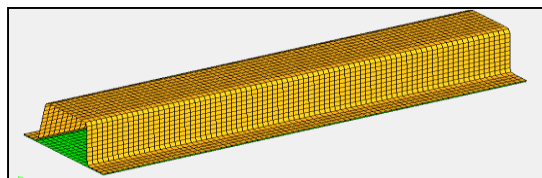


Figure 14: Cross section View of Iteration 5

Iteration 6 Details:

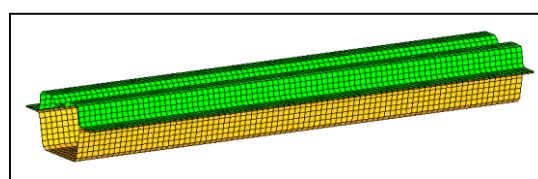


Figure 15: Cross section View of Iteration 6

Iteration 7 Details:

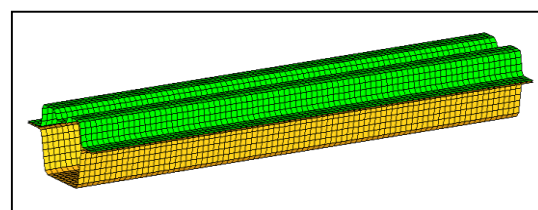


Figure 16: Cross section View of Iteration 7

3. RESULTS AND DISCUSSION

This section in elaborate discusses about the seven iterations performed with evaluation of the critical parameters like model deformation, Energy balance, section force.

Iteration 1:

The bumper rail cross section for iteration 1 is as shown in Fig 10. The Fig 17 shows the deformed view of the section at 108 msec

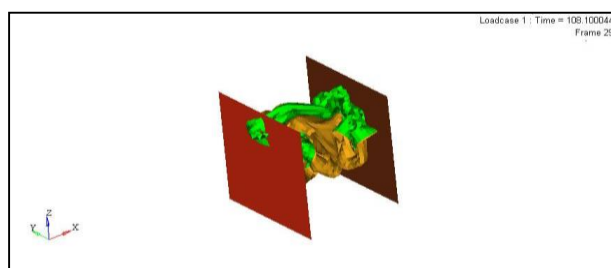


Figure 17: Iteration 1 model at Time=108 msec

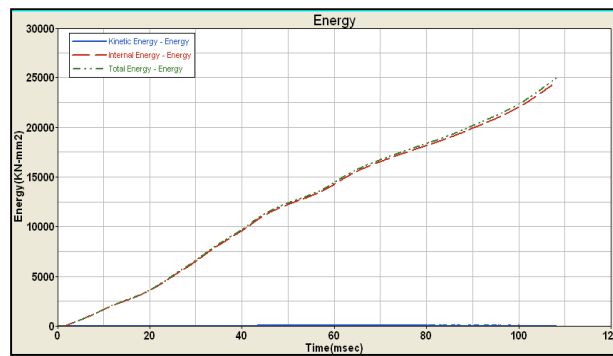


Figure 18: Energy curve distribution for Iteration 1

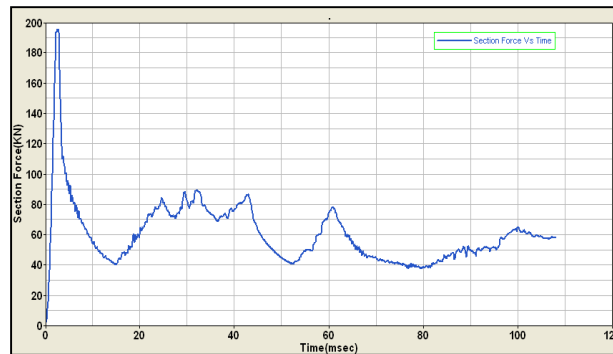


Figure 19: Force Curve for Iteration 1

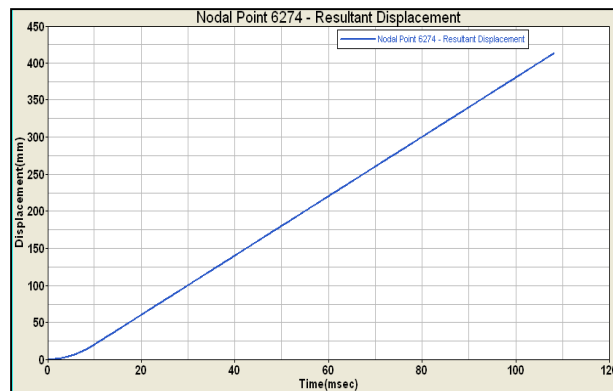


Figure 20: Displacement Curve for Iteration 1

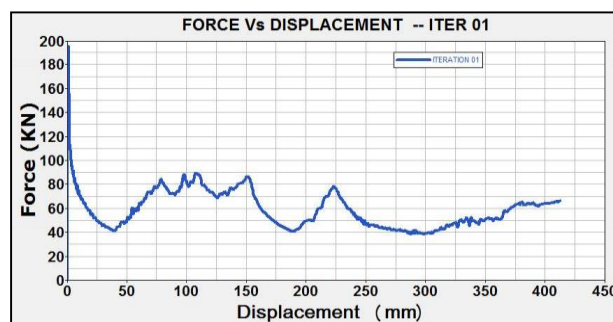


Figure 21: Force Vs Displacement (Energy Absorbed by Material) for Iteration 1

As observed from Fig 21, the Force displacement curve which is a measure of the work done on the bumper rail system or energy absorbed by the bumper rails, shows three identifiable peaks. Each peak signifies the each stage of rail crushing with energy absorption. We can also observe axial crushing in fig 17, of this design of the Bumper rail.

Iteration 2

The bumper rail cross section for iteration 2 is as shown in Fig 11. And also fig 22 shows the deformed view of the section at 108 msec

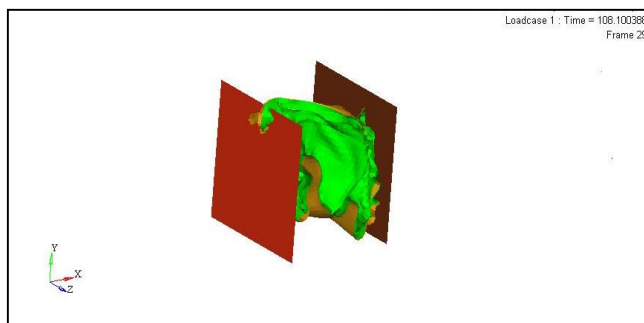


Figure 22: Iteration 2 model at Time=108 msec

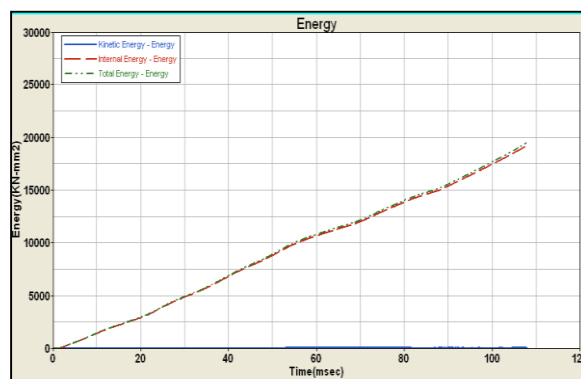


Figure 23: Global energy curves for Iteration 2



Figure 24: Force curve for Iteration 2

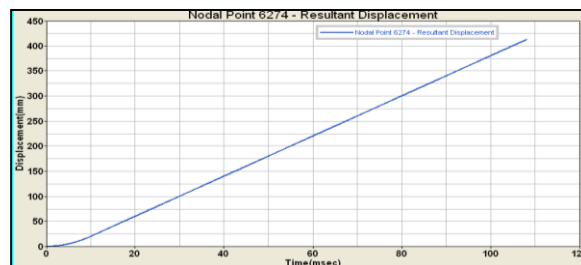


Figure 25: Displacement curve for Iteration 2



Figure 26: Force Vs Displacement (Energy Absorbed by Material) for Iteration 2

As observed from Fig 26, the Force displacement curve which is a measure of the work done on the bumper rail system or energy absorbed by the bumper rails, shows four identifiable peaks. Each peak signifies the each stage of rail crushing with energy absorption. We can also observe sideways buckling in fig.22, of this of the bumper rail.

Iteration 3

The bumper rail cross section for iteration 3 is as show in Fig 12. And also Fig 27 shows the deformed view of the section at 108 msec.

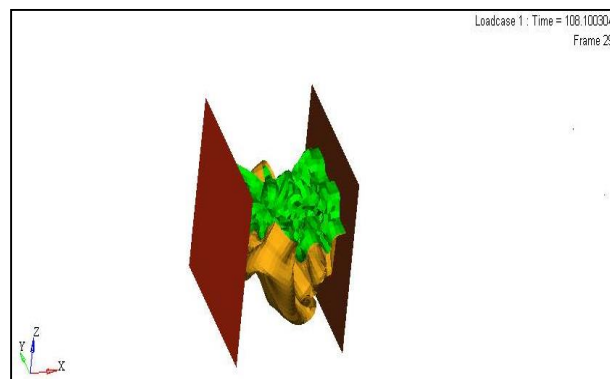


Figure 27: Iteration 3 model at Time = 108 msec

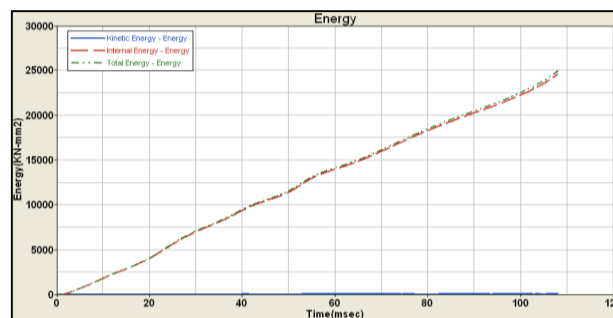


Figure 28: Global energy curves for Iteration 3

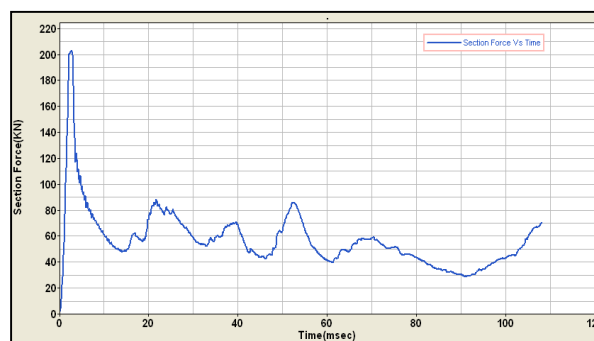


Figure 29: Force curve for Iteration 3

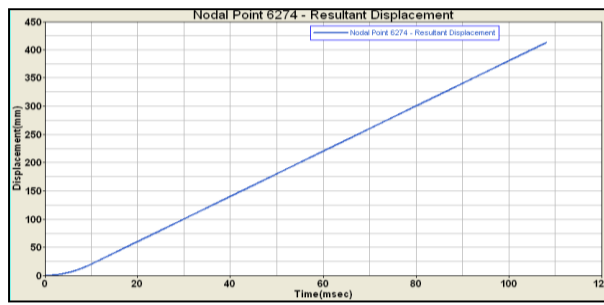


Figure 30: Displacement curve for Iteration 3

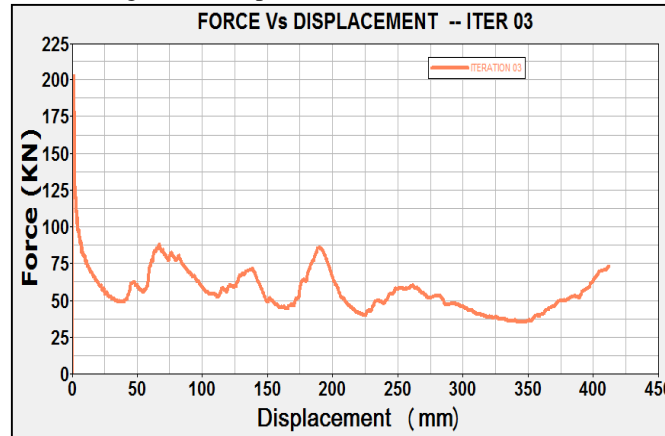


Figure 31: Force Vs Displacement (Energy Absorbed by Material) for Iteration 3

As observed from Fig 31, the Force displacement curve which is a measure of the work done on the bumper rail system or energy absorbed by the bumper rails, shows four identifiable peaks. Each peak signifies the each stage of rail crushing with energy absorption. We can also observe sideways buckling in fig 27, of this design of the Bumper rail.

Iteration 4

The bumper rail cross section for iteration 4 is as shown in Fig 13. And also Fig 32 shows the deformed view of the section at 108 msec.

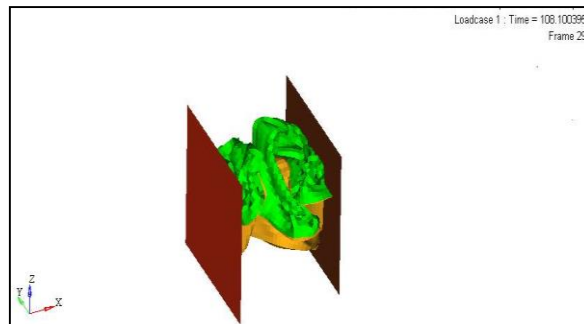


Figure 32: Iteration 4 model at Time=108 msec

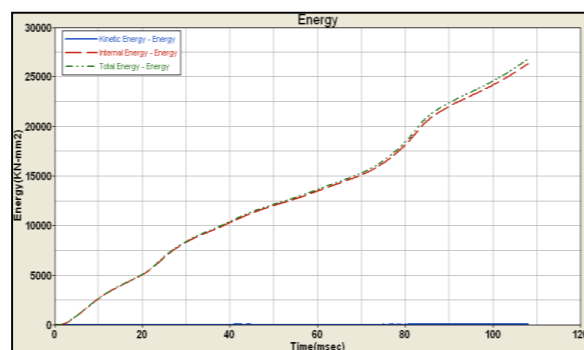


Figure 33: Global energy curves for Iteration 4

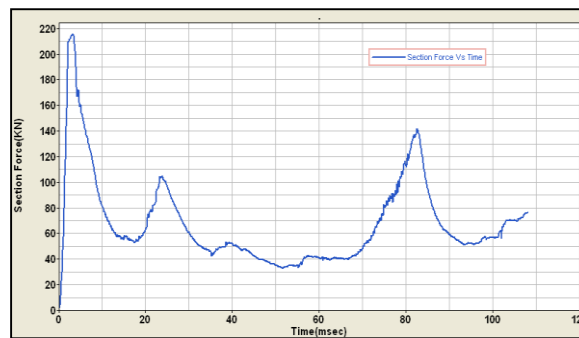


Figure 34: Force curves for Iteration 4

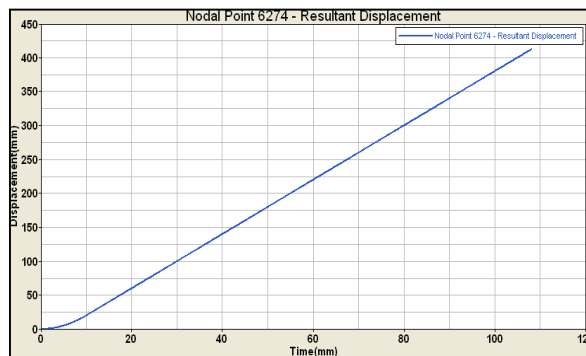


Figure 35: Displacement curves for Iteration 4

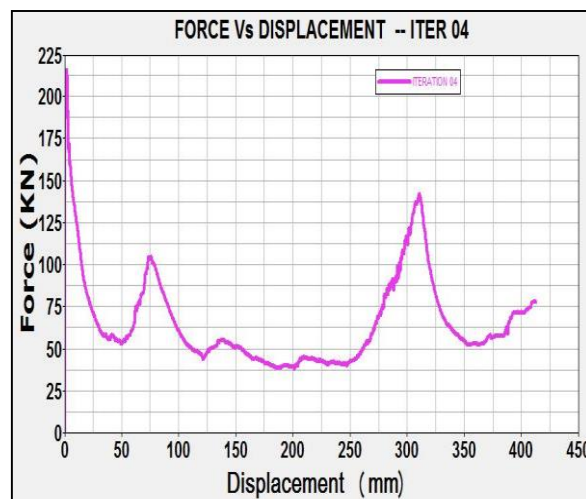


Figure 36: Force Vs Displacement (Energy Absorbed by Material) for Iteration 4

As observed from Fig 36, the Force displacement curve which is a measure of the work done on the bumper rail system or energy absorbed by the bumper rails shows three identifiable peaks. Each peak signifies the each stage of rail crushing with energy absorption. We can also observe complete axial crushing in fig. 32, of this design of the Bumper rail. The third peak at the later stage of the impact shows the presence of secondary crush mechanism in this design, which is desirable characteristic in the high speed impact.

Iteration 5

The bumper rail cross section for iteration 5 is as shown in Fig 14. And also Fig.37 shows the deformed view of the section at 108 msec

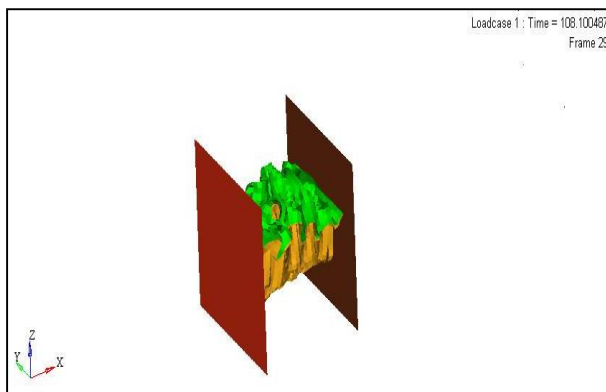


Figure 37: Iteration 5 model at Time = 108 msec

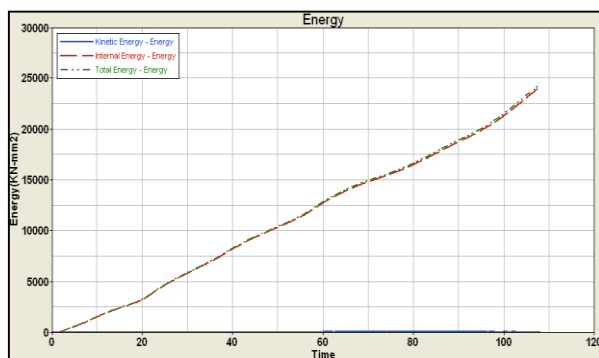


Figure 38: Global energy curves for Iteration 5

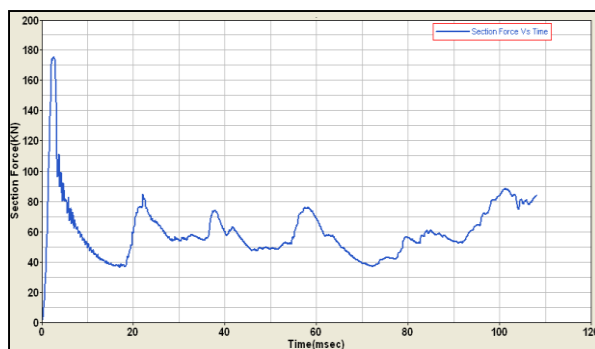


Figure 39: Force curve for Iteration 5

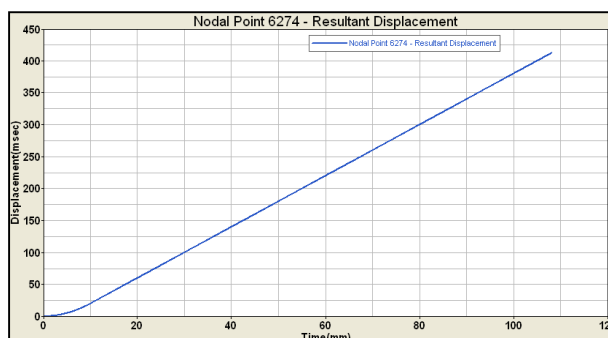


Figure 40: Displacement curve for Iteration 5

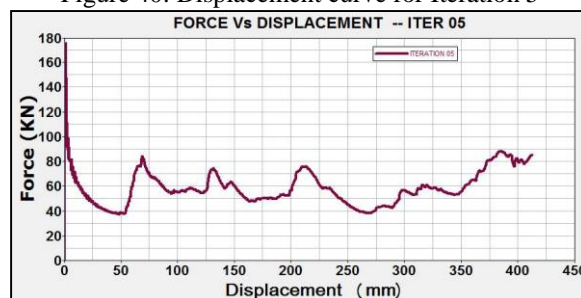


Figure 41: Force Vs Displacement (Energy Absorbed by Material) for Iteration 5

As observed from Fig 41, the Force displacement curve which is a measure of the work done on the bumper rail system or energy absorbed by the bumper rails, shows single large peak at the start of the impact and after that the energy absorption is more consistent. We can also observe axial crushing with material more clearly visible in fig 37, of this design of the Bumper rail.

Iteration 6

The bumper rail cross section for iteration 6 is as shown in Fig 15. And also Fig 42 shows the deformed view of the section at 108 msec.

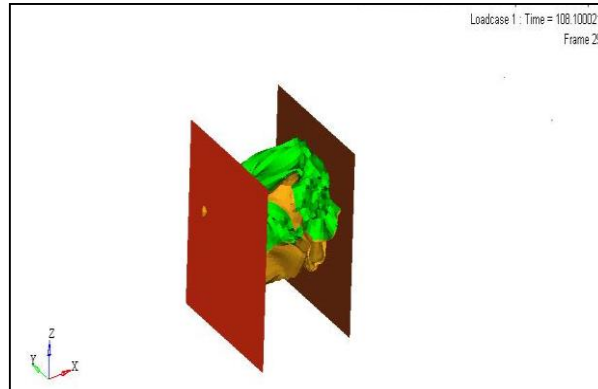


Figure 42: Iteration 6 model at Time = 108 msec

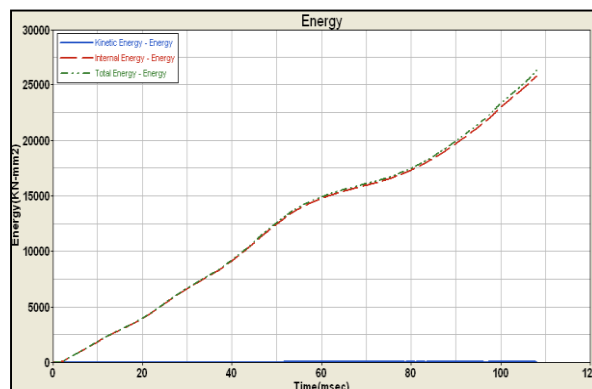


Figure 42: Global Energy curves for Iteration 6

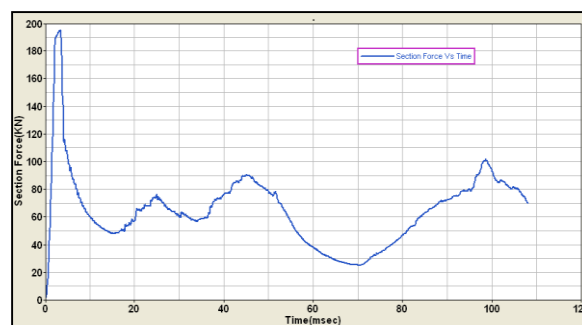


Figure 43: Force curve for Iteration 6

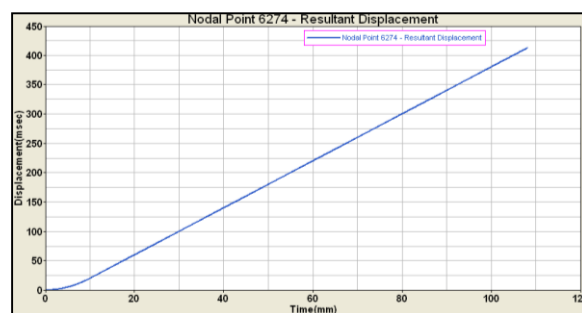


Figure 44: Displacement curve for Iteration 6

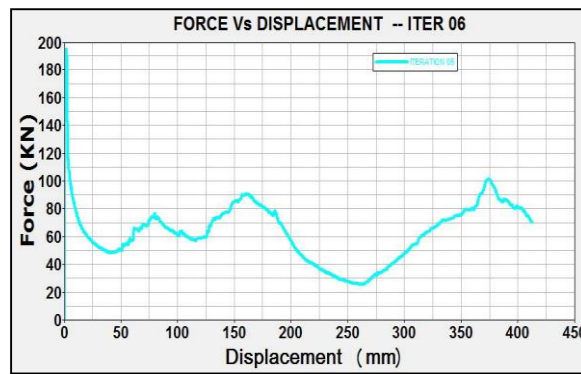


Figure 45: Force Vs Displacement (Energy Absorbed by Material) for Iteration 6

As observed from Fig 45, the Force displacement curve which is a measure of the work done on the bumper rail system or energy absorbed by the bumper rails shows two identifiable peaks. Each peak signifies the each stage of rail crushing with energy absorption. We can also observe sideways buckling in fig 42, of this design of the Bumper rail. The energy absorbed is more due to buckling of the rails than crushing.

Iteration 7

The bumper rail cross section for iteration 7 is as shown in Fig 16. And also Fig 46 shows the deformed view of the section at 108 msec

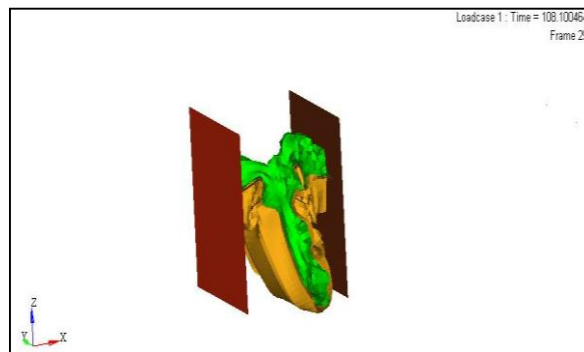


Figure 46: Iteration 7 model at Time = 108 msec

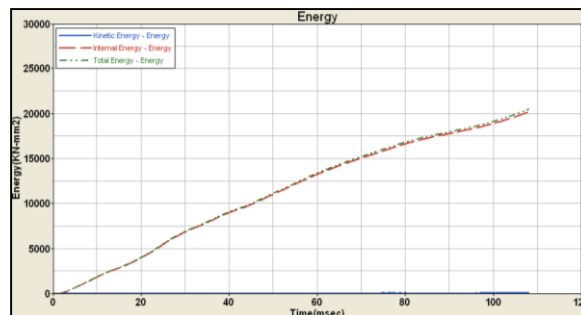


Figure 47: Global energy curves for Iteration 7

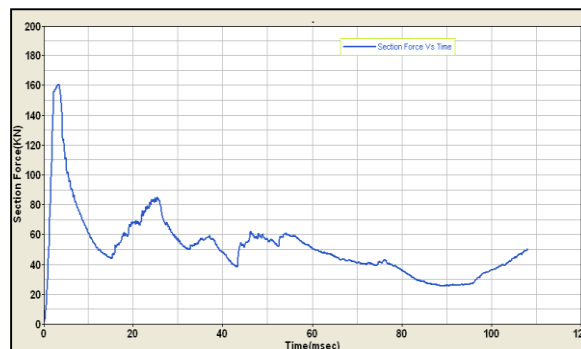


Figure 48: Force curve for Iteration 7

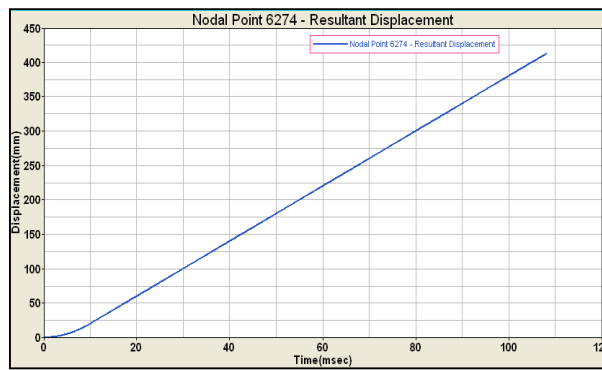


Figure 49: Displacement curve for Iteration 7

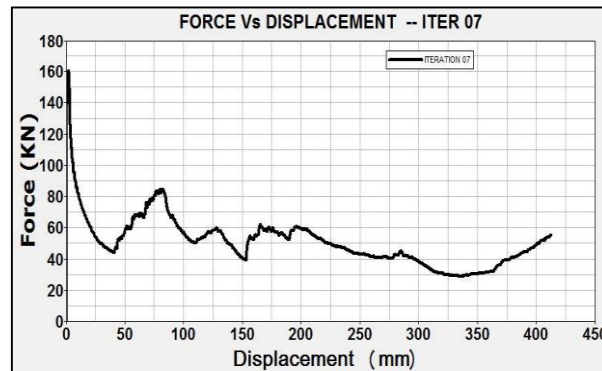


Figure 50: Force Vs Displacement (Energy Absorbed by Material) for Iteration 7

As observed from Fig 50, the Force displacement curve which is a measure of the work done on the bumper rail system or energy absorbed by the bumper rails shows two identifiable peaks. Each peak signifies the each stage of rail crushing with energy absorption. We can also observe downwards buckling in fig 46, of this design of the Bumper rail.

4. CONCLUSIONS

From the study performed, we have the following observations and conclusions:

- The figure 51 shows the F-D curves derived from seven iterations overlapped in a single curve. The design in iteration 4 has the most energy and also has the secondary crush characteristics. This design is more favorable from point of view of high speed impact. From the point of view of low speed impact, iteration 5 rail design is more favorable as there is more consistent energy absorption character with comparatively lower deformation.
- The general trend can be observed that with flat profile of the top rail, the axial crush characteristics are better, but with addition of features and section of top rail becoming more rectangular the buckling is more prominent than axial crush. This is basically due to addition of features to the total rail configuration and hence hindering axial crush.

10.2 COMPARISON BETWEEN ALL CURVES

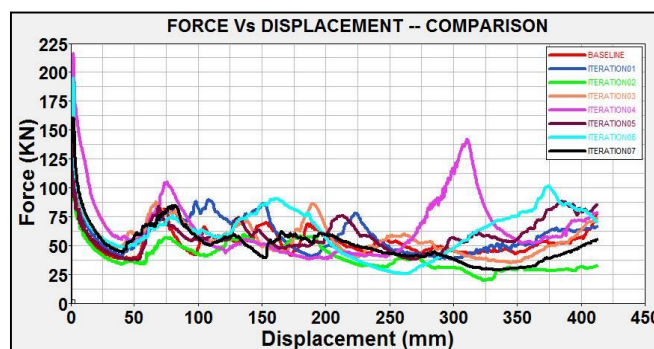


Figure 51: Force Vs Displacement curves of seven Iterations performed

REFERENCES

- [1] Matthew Avery, Motor Insurance Repair Research Centre, Joseph M.Nolan, Matthew Brumbelow and David S. Zuby, "Insurance Institute for Highway Safety Important Considerations in the Development of a Test to Promote Stable Bumper Engagement in Low Speed Crashes"
- [2] Sunan HUANG¹, Sweden Jikuang YANG¹Sweden Rikard, "Fredriksson optimization of design parameters for a contact sensor in bumper-pedestrian impact by using FE models".
- [3] Frschungsgesellschaft kraftfahrwesen mbh aachen angewandte forschung, entwicklung und consult, "Optimization of Bumper Systems"
- [4] Insurance Institute for Highway Safety. 2002. Low-Speed Crash Test Protocol: Version V. Arlington.
- [5] National Highway Traffic Safety Administration. 1999. Title 49 Code of Federal Regulations (CFR) Part 581, Bumper Standard. Washington, DC: Office of the Federal Register, National Archives and Records Administration.
- [6] Collapsible impact energy absorbers: an overview, A. A. A. Alghamdi, Department of Mechanical Engineering, King Abdulaziz University, PO Box 9027, Jeddah 21413, Saudi Arabia ,19 February 2001.
- [7] Research Council for Automobile Repairs. 1999. The Procedure for Conducting a Low Speed 15 km/h Offset Insurance Crash Test to Determine the Damageability and Repairability Features of Motor Vehicles.
Accessed: November 18, 2003.
- [8] Griškevičius, P. and Žiliukas, A. The impact energy absorption of the vehicles front structures, 2003.
- [9] Al Galib, D and Liman, A. Experimental and numerical investigation of static and dynamic axial crushing of circular aluminum tubes. Thin-Walled Structures, 2004
- [10] Metallic tube type energy absorbers: A synopsis A.G. Olabi Edmund Morris and M.S.J. Hashmi School of Mechanical and Manufacturing Engineering, Dublin City University, Dublin, Ireland, 25 July 2007
- [11] FOA (first-order analysis) model of a granule-filled tube for vehicle crash energy absorption by Dong Wook Lee, Zheng-Dong Ma and Noboru Kikuchi. Department of Mechanical Engineering, the University of Michigan, Ann Arbor, MI 48109, USA, December 2008.
- [12] Design and analysis of an automotive bumper beam in low-speed frontal crashes, Javad Marzbanrad, Masoud Alijanpour and Mahdi Saeid Kiasat School of Automotive Engineering, Iran University of Science & Technology, Narmak, Tehran, Iran, Department of Marine Technology, Amirkabir University of Technology, 15914 Tehran, Iran, 26 March 2009.